Turkish J. Eng. Env. Sci.
29 (2005) , 383 – 392.

Stress Analysis of a Cracked Finite Strip with Rigid Ends

Mehmet YETMEZ, Mehmet Ruşen GEÇİT
Middle East Technical University, Department of Engineering Sciences
Ankara-TURKEY
e-mail: gecit@metu.edu.tr

Received 12.07.2005

Abstract

A symmetrical finite strip containing a transverse symmetrical crack at the midplane is considered. Two rigid plates are bonded to the ends of the strip which are subjected to tensile axial loads. The material of the strip is assumed to be linearly elastic and isotropic. To verify the analytical solution provided previously by the authors, the problem is first solved numerically using a general purpose finite element code family MSC.MARC. Then, in order to see whether the verified results can be reproduced experimentally, laboratory tests are conducted according to the ASTM standards.

Key words: Finite strip, Crack, Finite elements, MSC.MARC, ASTM test methods.

Introduction

The systematic approach to the fracture behavior of brittle materials stems from the research by Griffith (1920) on the brittle fracture of glass, which laid the foundations of linear elastic fracture mechanics. The Griffith theory of fracture has been applied extensively to the fracture of metals, plastics and composites. Strip problems are of particular interest in engineering fracture mechanics. For this type of boundary value problem, analytical and numerical solutions are extensive. Analytical methods are generally based on integral equations (see Yetmez and Gecit (2005) or Yetmez (2002) for representative examples).

Among the numerical methods, the finite element method (FEM) dominates. Although other numerical methods give more accurate stress results (for example at the crack tip), its user friendly and available codes make the FEM useful for many academic and practical fracture mechanics analyses. One may conclude that for strips or panels designed to operate in the fractured area, isoparametric quadrilateral and constant strain triangular elements are efficient tools. In addition, it is clear that the whole strip structure may be analyzed using absolutely standard 8-noded elements. Harrop (1982) considered the optimum size of quarter-point crack tip elements. It was concluded that it is impossible to recommend a particular crack tip element size suitable for all situations. However, this is not the main problem in setting up a suitable finite element mesh. The emphasis so far has been on altering the crack tip element size while keeping all other aspects of the mesh the same. He realized that in setting up a mesh design one should aim at a balance between the representation of both singular and finite stress component terms. Any subsequent mesh refinement should retain this balance and in practice that implies adding elements. Normally extra elements are needed within a distance from the crack tip of the order of the net ligament and crack length. This assumes that the stress pattern in the uncracked body is already adequately represented. Details on the FEM of center-cracked plate problems are given by Yetmez (2002).

Notable developments in experimental fracture mechanics started with the evolution of ASTM test methods (see Yetmez (2002)). The standard test method ASTM E338 (1993) covers the determina-

tion of a comparative measure of the resistance of sheet materials to an unstable fracture originating from a very sharp stress-concentrator or crack. This test method is restricted to sheet materials not less than 0.64 mm and not exceeding 6 mm. The standard test method ASTM E399 (1997) is designed for the determination of the plane-strain fracture toughness of metallic materials by tests using a variety of fatigue-cracked specimens having a thickness of 1.6 mm or greater. The standard test method ASTM D5045 (1993) appears to characterize the toughness of plastics in terms of the critical stress intensity factor and critical strain energy release rate at fracture initiation. The significance of the standard and many conditions of testing are identical to those of ASTM E399 (1997).

With these ASTM methods and strain gage techniques, fracture analyses of any cracked strip may be determined. More information for well-defined strain gage applications in fracture research is available in full detail in Dally and Berger (1993).

Numerical Solution

A symmetrical finite strip with a length of $2L$ and a width of $2h$, containing a transverse symmetrical crack of width $2a$ at the midplane, has been considered by Yetmez and Gecit (2005). Two rigid plates are bonded to the ends of the strip, which are assumed to be subjected to axial tension of magnitude $P= 2hp_0$. The material of the strip is assumed to be linearly elastic and isotropic. Both edges of the strip are free of stresses. A solution to this finite strip problem is obtained by means of an infinite strip of width $2h$ that contains a crack of width $2a$ at $y = 0$ and 2 rigid inclusions of width $2c$ at $y = \pm L$ and that is subjected to uniformly distributed axial tensile loads of magnitude $P= 2hp_0$ at $y = \pm\infty$. Field equations of the linear elasticity theory are solved subject to the following boundary conditions:

$$\sigma_y(x, \pm\infty) = p_0 \tag{1}$$

$$\sigma_y(x, 0) = 0\,, \quad (|x| < a) \tag{2}$$

$$\sigma_x(\pm h, y) = 0\,, \quad \tau_{xy}(\pm h, y) = 0 \tag{3a,b}$$

$$u(x, \pm L) = 0\,, \quad v(x, \pm L) = \text{ constan } t\,, \quad (|x| < c) \tag{4a,b}$$

in which σ and τ denote normal and shearing stresses, and u and v denote the displacements. General expressions containing a sufficient number of unknowns are obtained by use of Fourier sine/cosine transforms alternately in the x and y directions. Expressions satisfying (1) and (3) contain 3 unknowns, namely the crack surface displacement derivative

$$m(x) = \frac{1}{2}\frac{\partial}{\partial x}\left[v\left(x, 0^+\right) - v\left(x, 0^-\right)\right] \tag{5}$$

and the jumps in the stresses through the inclusions

$$p_1(x) = \tau_{xy}\left(x, L^+\right) - \tau_{xy}\left(x, L^-\right) \tag{6}$$

$$p_2(x) = \sigma_y\left(x, L^+\right) - \sigma_y\left(x, L^-\right) \tag{7}$$

These unknown functions are calculated by solving 3 singular integral equations resulting from the boundary conditions on the crack and the inclusions. When the width of the rigid inclusions approaches the width of the strip, i.e. when $c \to h$, the portion of the infinite strip between the rigid inclusions becomes identical with the finite strip problem. The unknown functions m, p_1 and p_2 are singular at $x = \pm a$ and $x = \pm h$, respectively:

$$m(x) = M(x)\Big/\left(a^2 - x^2\right)^{\alpha}\,, \quad 0 < Re(\alpha) < 1 \tag{8}$$

$$p_i(x) = P_i(x)\Big/\left(h^2 - x^2\right)^{\beta}\,, \ (i = 1, 2)\ , \ 0 < Re(\beta) < 1 \tag{9a,b}$$

where M, P_1 and P_2 are Hölder-continuous functions in the respective intervals.

The strength of the singularities may be calculated if the integral equations are examined near the end points using the complex function technique described by Muskhelishvili (1953) and the procedure given by Cook and Erdogan (1972):

$$\alpha = 1/2,\ 2\kappa\cos\pi\beta + 4(\beta - 1)^2 - \kappa^2 - 1 = 0 \tag{10a,b}$$

where

$$\kappa = 3 - 4\nu \text{ for plane stress} \tag{11}$$

$$\kappa = (3 - \nu)/(1 + \nu) \text{ for plane strain} \tag{12}$$

with ν being Poisson's ratio. The singular integral equations are reduced to a system of linear algebraic equations, using the Gauss-Jacobi and the Gauss-Lobatto integration formulas (Erdogan et al., 1973; Krenk, 1975), which is solved numerically. Afterwards, all quantities of practical interest can be calculated numerically.

Now consider a finite strip with a length of $2L$ and a width of $2h$, containing a transverse symmetrical crack of width $2a$ at the midplane. Two rigid plates are bonded to the ends of the strip, which are assumed to be subjected to axial tension of magnitude

$P = 2hp_0$. The material of the strip is assumed to be linearly elastic and isotropic. If one imagines fixed grip conditions, the formal boundary conditions of the linear elasticity problem will be Eqs. (2), (3a) and (3b) and

$$u(x, \pm L) = 0\,, \quad v(x, \pm L) = v_0\,, \qquad (|x| < h) \tag{13a,b}$$

where (see Yetmez (2002))

$$v_0 = \frac{\kappa + 1}{16\mu}\frac{L}{h}P\,, \tag{14}$$

μ is the shear modulus.

For a numerical solution of the problem, a cracked finite strip model with high mesh density is considered. Referring to Harrop (1982), 8-noded quadrilateral plane stress/strain full integration elements are used to provide successful performance for both crack tip and inclusion edge singularities. The range of converged singularity ratios for the analyses is presented. The numerical results obtained are compared with the analytical solutions. A specific crack element is briefly discussed for its capacity to obtain accurate results with a coarse mesh. Throughout the numerical solution of a cracked finite strip (Figure 1), the general purpose finite element code MSC.MARC, with its pre- and post-processor MSC.MARC MENTAT, is used. In order to analyze the stress field of the strip with a reasonable accuracy, fine meshed models are used for various strip and crack geometries. Due to symmetry, only one-fourth of the cracked finite strip (Figure 2) needs to be modeled.

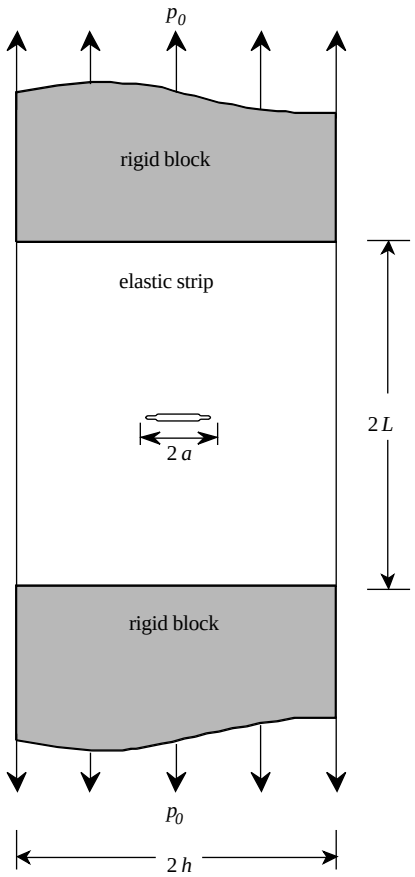

Figure 1. General illustration of a cracked finite strip.

In order to determine the stress field of a cracked finite strip, the finite element model shown in Figure 2 is used (see Yetmez (2002)). The model involves focusing a tremendous amount of attention on the crack tip and the inclusion edge in order to obtain the stress field accurately. The primary objective of the analysis of the cracked finite strip is the calculation of appropriate normal and shearing stresses in the vicinity of both the crack tip and inclusion edge. Therefore, highly refined meshes are to be defined and used to represent the singularities properly and to obtain reasonably correct stress distributions in the strip. Given in Figure 2, the optimum mesh can be obtained by a trial and error procedure. The procedure indicates that an inclusion length of $L/10$ is sufficient for the analysis. The MSC.MARC 8-node distorted quadrilateral elements, QUAD8, are used

for the cracked finite strip analysis. The singularity in QUAD8 is achieved by placing the mid-side node near the crack tip and the inclusion edge. The mesh characteristics of the 8-node quadrilateral plane element model are given in Table 1.

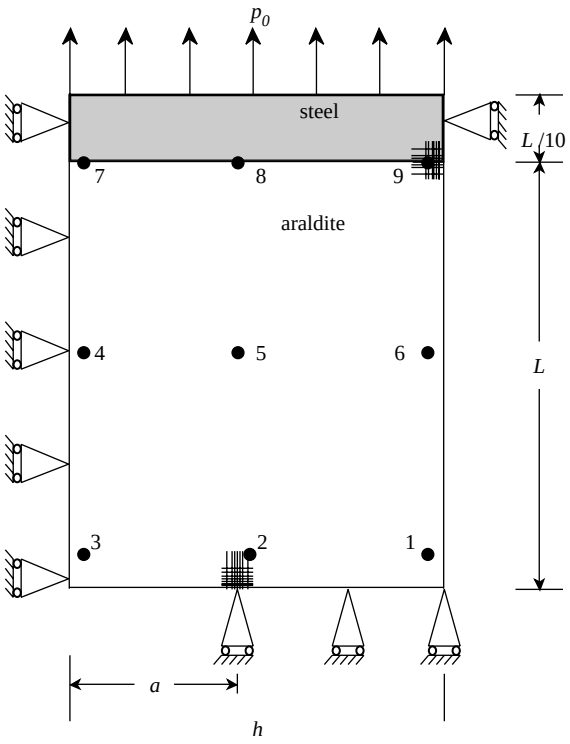

Figure 2. Finite element model and gage installation nodes.

Boundary conditions for the model are determined by symmetry conditions. The whole left edge along the axial direction is constrained in the transverse direction. The right edge along the inclusion in the axial direction is also constrained in the transverse direction. The edge along the crack is constrained in the axial direction. Thus, the unit load $p_0 = P/2h$ is applied along the far edge of the inclusion as a uniform negative pressure. In all the models, element thickness is equal to 1. Material properties of the finite element model: (1) Young's modulus, $E = 2 \times 10^{11}$ N/cm^2, Poisson's ratio $\nu = 10^{-3}$ for the rigid inclusion, and (2) $E = 2 \times 10^7$ N/cm^2, $\nu = 0.01$-0.49 for the strip.

Experimental Work

The main goal or expectation of this part is to determine the experimental behavior of the cracked finite strips at small strain levels. In order to determine the test method and its rudimentary sequences of such strips including their loading and boundary conditions, ASTM test standards are taken into consideration. After selecting the materials and installing devices, such as machines and strain gages, 8 cracked finite strip specimens are tested and both numerical and pictorial data are obtained. All analytical, numerical and experimental results are compared graphically.

The cracked finite strip specimens consist of 2 types of material. A low-carbon steel and a dimensionally stable, stiff polymer are used for the inclusion and the strip materials, respectively. The low-carbon steel, ERDEMIR ST 3237 A1, or shortly ERD 3237, is produced by Eregli Iron and Steel Works Co., Turkey. On the other hand, the polymer, ARALDITE, is produced by CIBA Specialty Chemicals Inc., Switzerland. These 2 types of material are assumed to be linearly elastic and isotropic. Their mechanical properties are given in Table 2. Eight cracked finite strip specimens are prepared by considering the standard ASTM E338 (ASTM E338

Table 1. Refined mesh characteristics for the quarter cracked finite strip models.

	$a = 0$		$a = 0.01h$		$0.01h < a < 0.99h$		$a = 0.99h$	
L/h	Node #	Elem. #	Node #	Elem. #	Node #	Elem. #	Node #	Elem. #
0.25	5353	1728	9737	3168	8471	2752	9053	2944
0.5	5243	1692	13043	4260	8078	2623	9053	2944
1	5529	1786	10248	3337	8633	2806	9635	3136
2	5815	1880	10893	3550	9188	2989	10217	3328
4	6101	1974	11538	3763	9743	3172	10799	3520
8	6387	2068	12183	3976	10298	3355	11381	3712

1993) as shown in Figure 3. By starting with central slots, cracks with sharp ends are prepared according to the standard ASTM D5045 (ASTM D5045 1993). Finally, strain gages are glued to the strip specimens (see Yetmez (2002)). For the purpose of strain measurements in the x- and y-directions, 5 mm foil resistance strain gages and an adhesive are used. The FLA-5-11 strain gages (gage factor: 2.13 $\pm$ 0.01 and gage resistance: 120 $\pm 0.3\Omega$) are products of TML, Tokyo Sokki Kenkyojo Co., Ltd., Japan. The adhesive is produced by Bison Power Glue, Holland. Throughout the experimental procedure, measurements are taken on one-fourth of the specimens ($0 < x < h, 0 < y < L$) only. The unidirectional strain gages are mounted by considering 9 critical points on this fourth. The sequence of the gage installation is shown in Figure 2.

Static tension tests are performed such that the cracked finite strip specimens are under small strain conditions, i.e. $\varepsilon \leq 0.3\%$. Therefore, a constant axial tensile load of 700 N is applied. For the strain measurements in the principal directions, a minimum 2 mm/min loading rate is used to reach the applied maximum load, 700 N, using a computer aided screw-driven testing machine, Lloyd LS500 (Lloyd Instruments, UK). NEXYGEN 2.0 software (Lloyd) is used for this purpose.

The 9-channel strain measurements are completed using a Portable Strain Indicator with its Switch and Balance Unit (Model: P-350A, Vishay Instruments, Vishay Measurement Group, USA). Prior to the measurements, it is observed that temperature effects in the actual strain gages cause significant changes in resistance, which can lead to erroneous readings. Therefore, a convenient method of temperature compensation is used. For this purpose, one specimen is used as the dummy, while the other is tested as the active one.

Cracked finite strip specimens may be assumed to be under plane stress conditions. Therefore, formulas of plane stress state are used:

$$\sigma_x = \frac{E}{1-\nu^2}\{\varepsilon_x + \nu\varepsilon_y\} \tag{15}$$

$$\sigma_y = \frac{E}{1-\nu^2}\{\varepsilon_y + \nu\varepsilon_x\} \tag{16}$$

where E is the Young's modulus and ε denotes normal strain.

Results

The cracked finite strip is completely defined by the dimensionless parameters L/h, a/h and Poisson's ratio ν. In the numerical work, instead of ν, κ defined in Eqs. (11) and (12) is used. Thus, the numerical results obtained for one particular value of the material constant κ can be used for plane strain or plane stress geometry with the corresponding Poisson's ratio calculated from Eq. (11) or (12). Distances and stresses are normalized with the width of the strip,

Table 2. Mechanical properties of the selected materials.

Material	ρ (g/cm^3)	E (GPa)	ν	σ_{yield} (MPa)
ERD 3237	7.86	207	0.3	288
ARALDITE	1.61	1.04	0.35	43.33

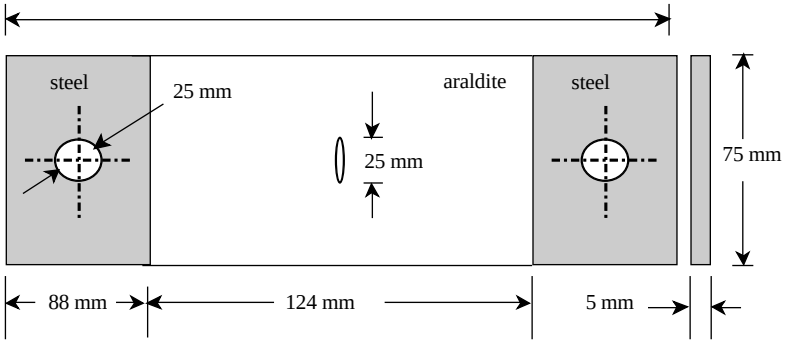

Figure 3. Details of a cracked finite strip specimen according to ASTM E338-93.

h, and the mean value of the axial load applied to the strip, $p_0 = P/2h$. For numerical solution a cracked finite strip model with high mesh density is considered. Eight-noded quadrilateral plane stress/strain full integration elements are used to provide successful performance for both crack tip and inclusion edge singularities. The numerical results obtained are compared with the analytical solutions. A specific crack element is briefly discussed for its capacity to obtain accurate results with a coarse mesh. Some of the computed results for $a/h = 0.5$ are shown in Figures 4-10, together with the results of the analytical solution for verification. It can be seen that there is an almost perfect agreement between the results of the analytical and numerical solutions.

Figures 4-7 show normal and shearing stress distributions at $y = L$. In these figures, $L = h$ or $8h$; $\nu = 0.3$ (plane strain), 0.42857 (plane stress); and $a = 0.5h$. There is a better agreement between analytical and numerical results when the aspect ratio L/h increases. Note also that the stresses become infinity at the corner $x = h$, $y = L$.

Eight cracked finite strip specimens are tested and both numerical and pictorial data are obtained (see Yetmez (2002)). All analytical, numerical and experimental results are compared graphically. The average values of the strains for the 8 specimens with their measurement nodes are given in Table 3. No ε_x measurement is obtained at nodes 7, 8 or 9. This is due to the fact that there will be negligibly small ε_x values at nodes 7, 8 and 9, which are very close to the rigid plate (ERD3237). Hence, it is assumed that ε_x at these nodes is zero without obtaining measurements.

Experimental stress distributions calculated from Eqs.(15) and (16) are compared with related analytical and numerical results. The analytical, numerical and experimental results are presented graphically in Figures 8-10. These figures show that the experimental findings are acceptable since they have the same trends as the analytical or numerical results, but always give somewhat smaller values for the stresses. This may partly be due to unavoidable deformations in the adhesive used to fasten the strain gages to the specimens. Experimental results slightly on the lower side may be due to the use of relatively long strain gages also.

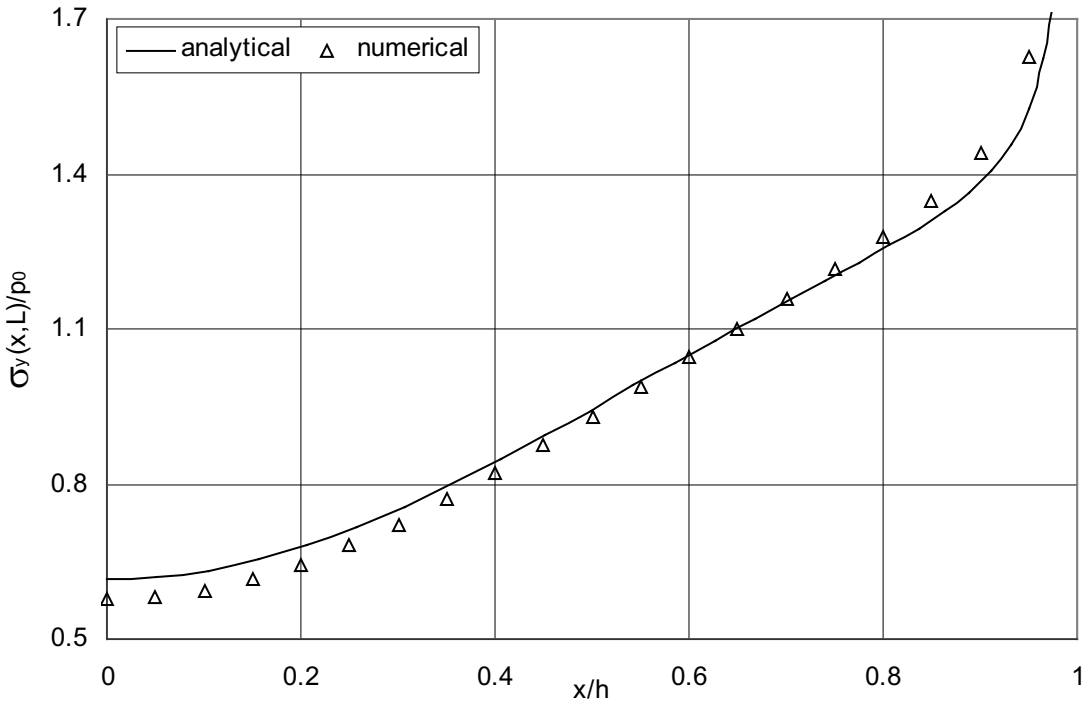

Figure 4. Normal stress σ_y at $y = L$ for $L = h$, a= $0.5h$; $\nu = 0.3$ (plane strain) or $\nu = 0.42857$ (plane stress).

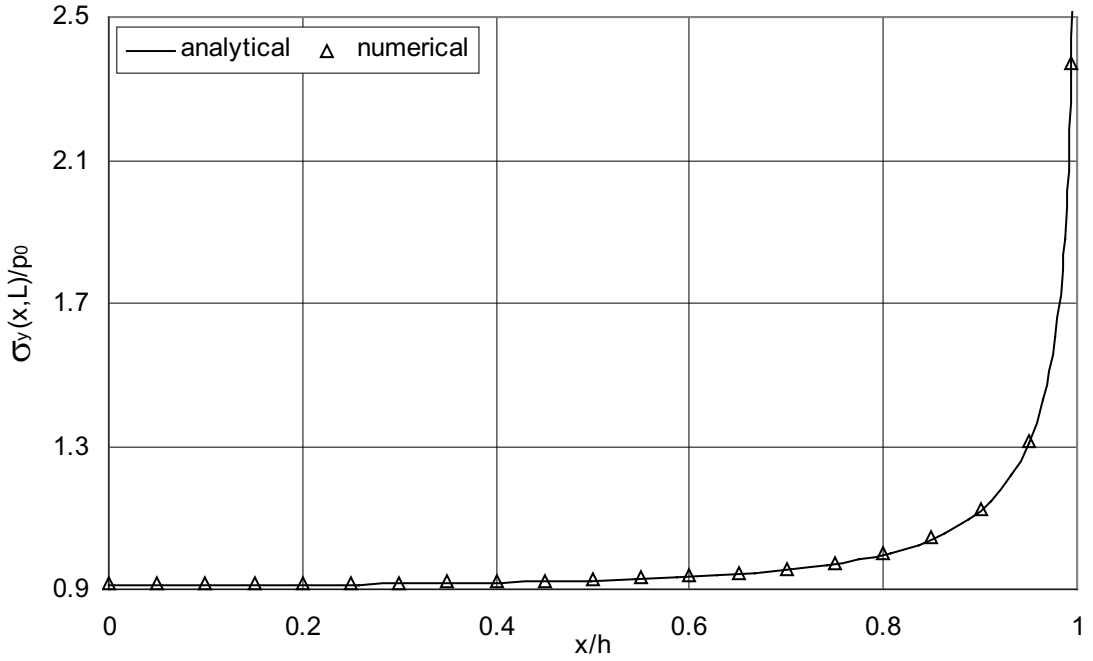

Figure 5. Normal stress σ_y at $y = L$ for $L = 8h$, $a = 0.5h$; $\nu = 0.3$ (plane strain) or $\nu = 0.42857$ (plane stress).

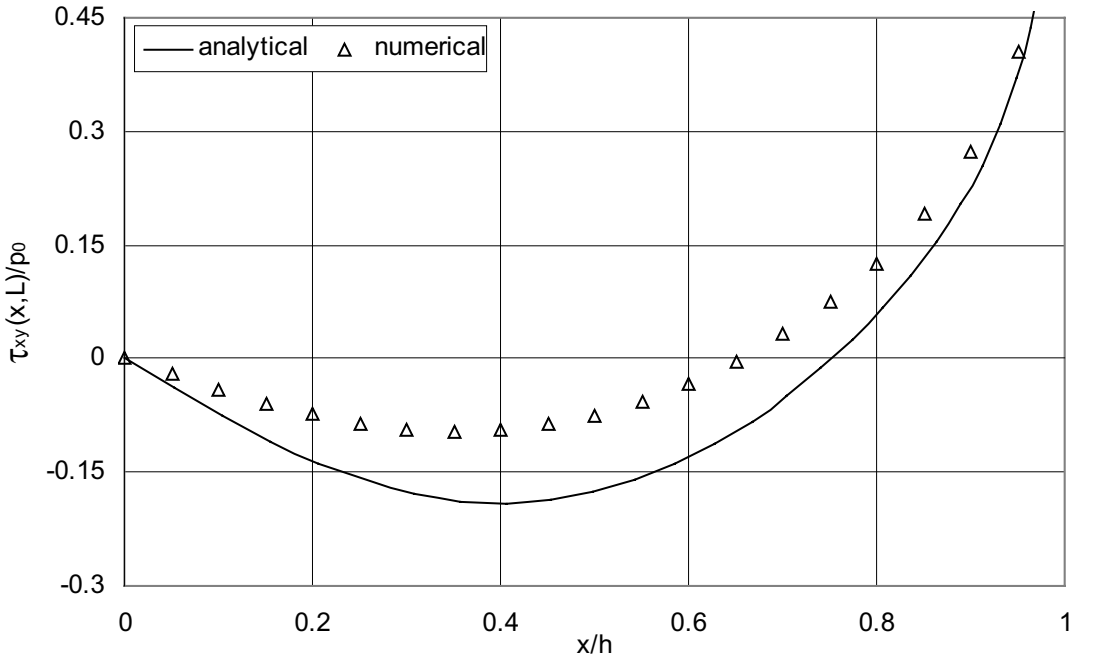

Figure 6. Shearing stress τ_{xy} at $y = L$ for $L = h$, $a = 0.5h$; $\nu = 0.3$ (plane strain) or $\nu = 0.42857$ (plane stress).

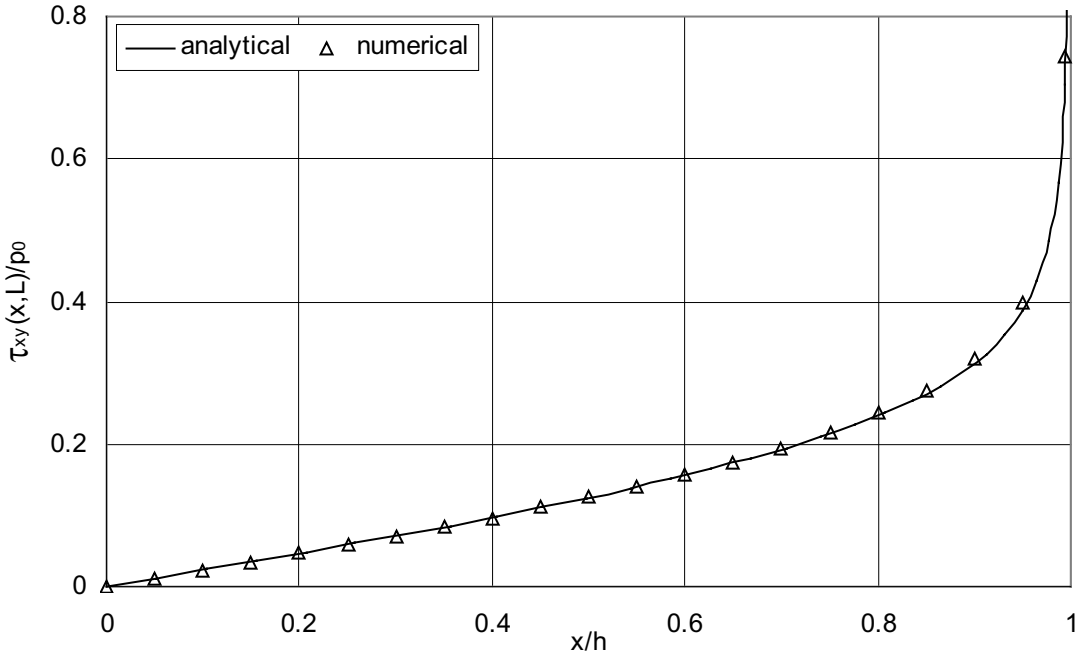

Figure 7. Shearing stress τ_{xy} at $y = L$ for $L = 8h$, $a = 0.5h$; $\nu = 0.3$ (plane strain) or $\nu = 0.42857$ (plane stress).

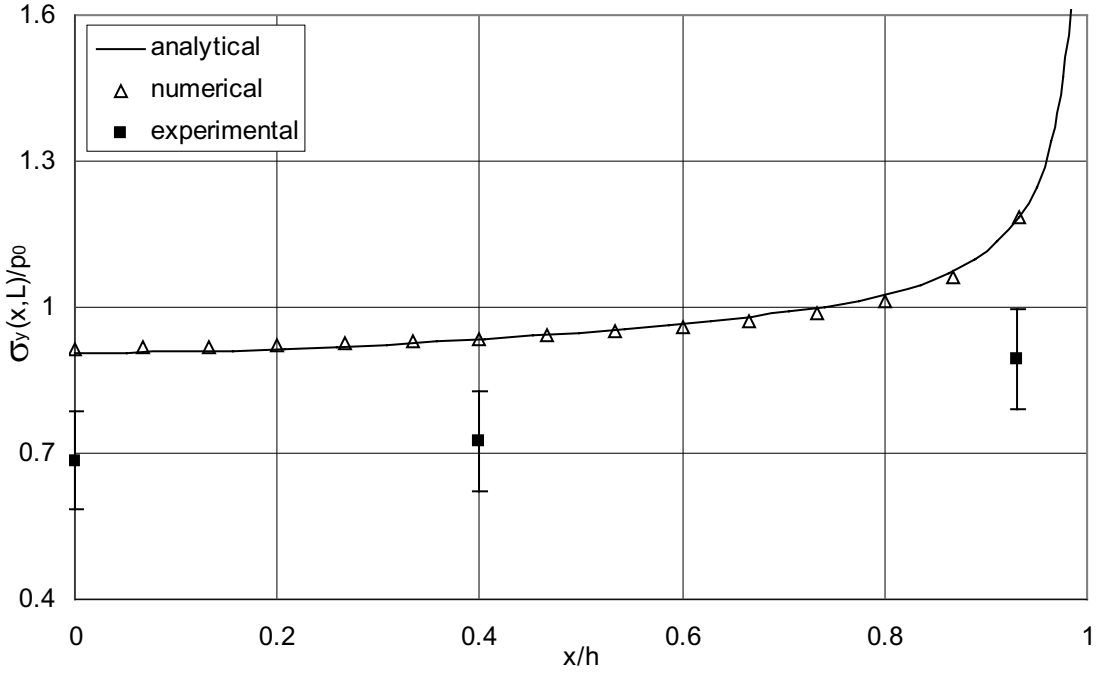

Figure 8. Normal stress σ_y at $y = L$ for $L = 1.653h$, $a = 0.333h$; $\nu = 0.35$ (plane stress).

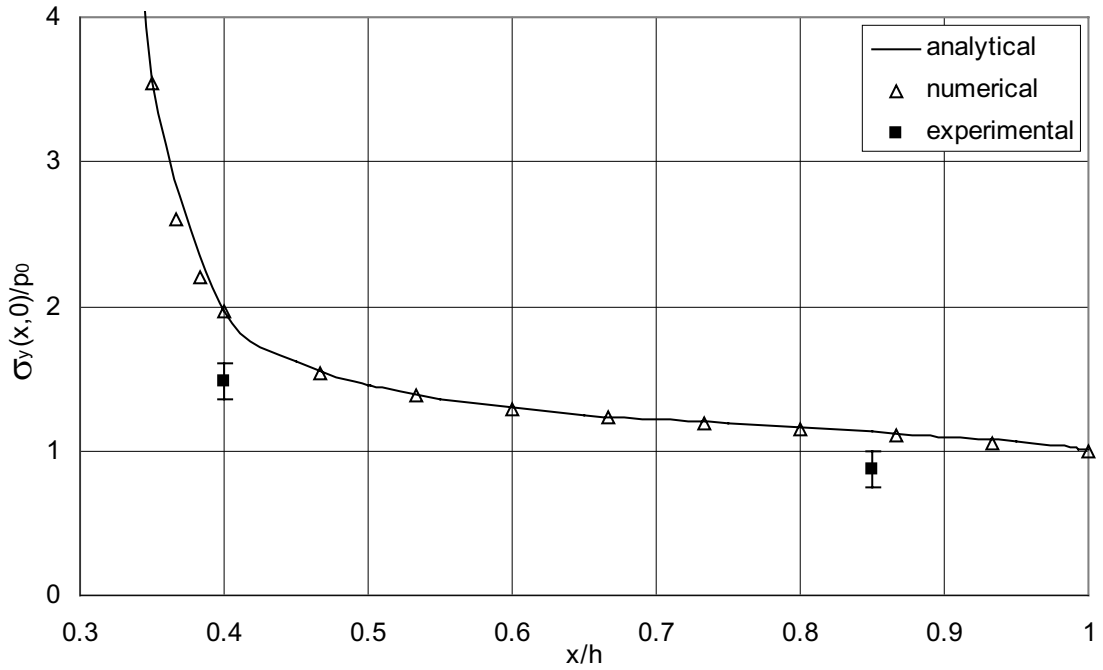

Figure 9. Normal stress σ_y at $y = 0$ for $L = 1.653h$, $a = 0.333h$; $\nu = 0.35$ (plane stress).

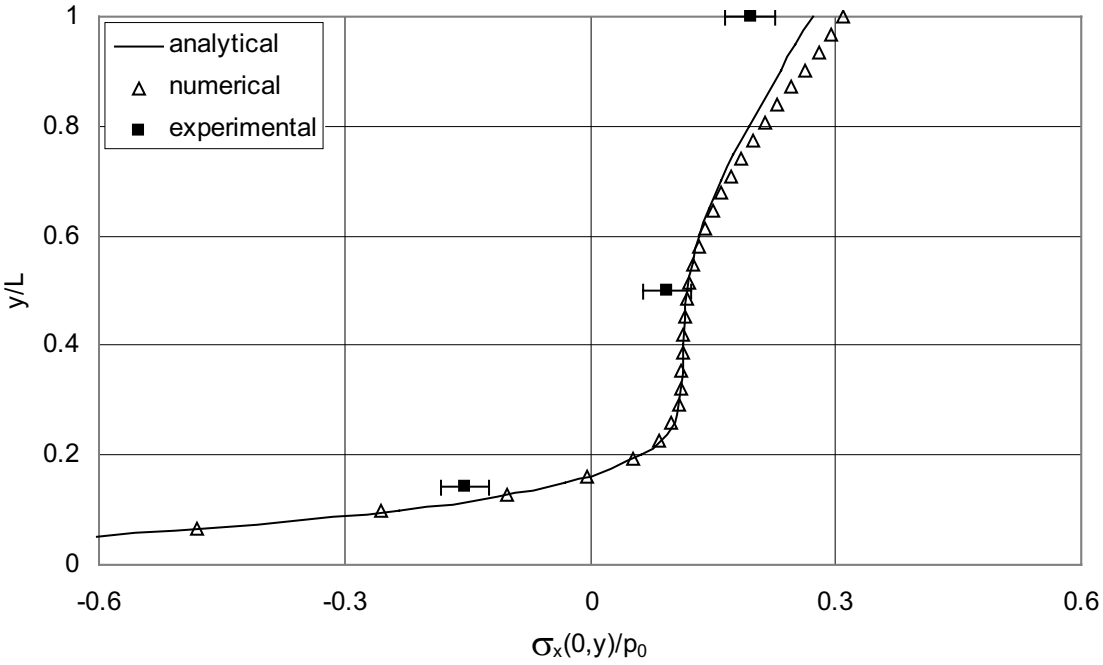

Figure 10. Normal stress σ_x at $x = 0$ for $L = 1.653h$, $a = 0.333h$; $\nu = 0.35$ (plane stress).

Table 3. Averaged strain measurements of 8 cracked finite strip specimens.

Node #	ε_x (μstrain)	ε_y (μstrain)
1	-512	1145
2	-342	2038
3	-583	181
4	-348	1116
5	-523	1158
6	-539	1094
7	-	767
8	-	772
9	-	1289

Nomenclature

L	half length of finite strip
h	half width of finite strip
a	half width of crack
c	half width of rigid inclusions
P	axial load applied to the rigid end plates
p_0	mean axial normal stress
u	transverse displacement
v	axial displacement
ρ	material density
ε	normal strain
σ	normal stress
σ_{yield}	yield stress
τ	shearing stress
E	Young's modulus
ν	Poisson's ratio
M,P_1,P_2	Hölder-continuous density functions
μ	shear modulus

References

ASTM D5045-91a, "Standard Test Method for Plane-Strain Fracture Toughness and Strain Energy Release Rate of Plastic Materials", Annual Book of ASTM Standards, ASTM, 08.03, 314-322, 1993.

ASTM E338-93, "Standard Test Method of Sharp-Notch Tension Testing of High-Strength Sheet Materials", Annual Book of ASTM Standards, ASTM, 03.01, 462-467, 1993.

ASTM E399-97, "Standard Test Method for Plane-Strain Fracture Toughness of Metallic Materials", Annual Book of ASTM Standards, ASTM, 03.01, 509-539, 1997.

Cook, T.S. and Erdogan, F., "Stresses in Bonded Materials with a Crack Perpendicular to the Interface", International Journal of Engineering Science, 10, 677-697, 1972.

Dally J.W. and Berger J.R., "The Role of the Electrical Resistance Strain Gauge in Fracture Research", Experimental Techniques in Fracture, (ed. Epstein, J.S.), Society of Experimental Mechanics, Bethel, CT, 1-37, 1993.

Erdogan, F., Gupta, G.D. and Cook, T.S., "Numerical Solution of Singular Integral Equations", Methods of Analysis and Solutions of Crack Problems, (ed. Sih G.C.), Noordhoff International Publishing, Leyden, The Netherlands, 1973.

Griffith A.A., "The Phenomena of Rupture and Flow in Solids", Journal of Philosophy Transactions of the Royal Society London, A.221, 163-198, 1920.

Harrop, L.P., "The Optimum Size of Quarter-Point Crack Tip Elements", International Journal of Numerical Methods and Engineering, 18, 1101-1103, 1982.

Krenk, S., "On the Elastic Strip with an Internal Crack", International Journal of Solids and Structures, 11, 693-708, 1975.

Muskhelishvili, N.I., Singular Integral Equations, Noordhoff Publishing Corp., Groningen, Holland, 1953.

Yetmez M., Analytical, Numerical and Experimental Solutions of a Cracked Finite Strip, PhD Dissertation, Ankara, Turkey: Department of Engineering Sciences, Middle East Technical University, 2002.

Yetmez M. and Gecit M.R., "Finite Strip with a Central Crack under Tension", International Journal of Engineering Science, 43, 472-493, 2005.